

On the Wave Character of the Electron

G. Poelz

Abstract—A classical model of the electron based on Maxwell's equations is presented in which a circulating massless electric charge field moves in a spherical background field maintained by the synchrotron radiation of the charge. It yields the de Broglie wave character of the electron and the magnetic moment yields the size of the object. Superpositions of solutions of the electromagnetic wave equations lead to finite angular momentum and total energy. It is the movement with speed of light which makes the electron mass equivalent to the electric and magnetic field energies.

Keywords—Electron, mass, spherical wave field, wave model.

I. INTRODUCTION

ELECTRICAL effects are known for several hundred years. The electron, as particle, has been discovered already at the end of the 19th century [1] and fascinates since then by its properties. It plays a fundamental role in the structure of matter, and in science like physics and chemistry. Technical designs are dominated today by its applications.

The properties of the electron are summarized as follows:

- The electron has an elementary charge $Q = -e$ with a point-like structure. This is expressed by an electric field which is described by the Coulomb field sketched in Fig. 1.

$$\mathcal{E} = \frac{e}{4\pi\epsilon_0 \cdot r^2} . \quad (1)$$

The problem of the singularity at the origin is usually removed just by a truncation at the classical electron radius r_e , by replacing the point charge by a charge distribution with radius r_e , or by modifying the electric permittivity ϵ_0 appropriately.

- It has a magnetic dipole moment

$$M = \frac{e}{2m_e} \cdot \frac{\hbar}{2} \cdot 2.0024 \quad (2)$$

which suggests a circulating charge like in Fig.2.

- The electron owns an intrinsic angular momentum, the spin, with

$$L_s = \frac{1}{2}\hbar . \quad (3)$$

- It has a finite rest mass

$$m_e = 9.11 \cdot 10^{-31} [kg] . \quad (4)$$

- It shows a wave like behavior at small distances defined 1924 by L. de Broglie [2]. Its wave length λ is related to its momentum p by

$$\lambda = \frac{2\pi\hbar}{p} . \quad (5)$$

retired from Hamburg University, Institute of Exp. Physics, Hamburg, Germany; e-mail: poelz@mail.desy.de
submitted to Int. J. of Mathematical, Physical and Engineering Sciences in an earlier version, April 15, 2009

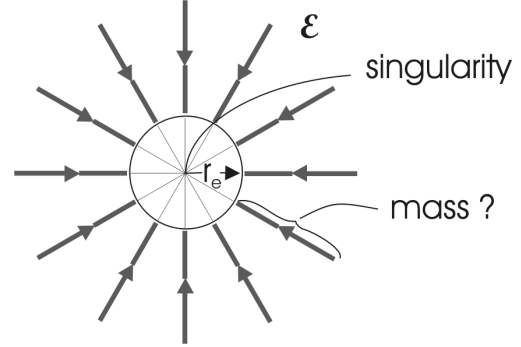


Fig. 1. Classical picture of the electron. The electric field points to the charge in the center. The Coulomb field is truncated at r_e , such that the energy of the residual field corresponds to the mass.

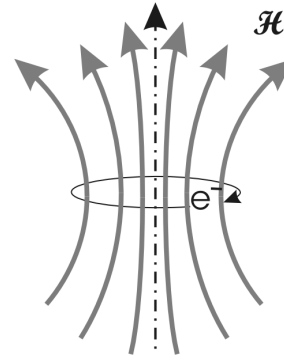


Fig. 2. The magnetic moment of the electron suggests a current to be present

- From interactions at low and medium energies the Compton wavelength $\lambda_C = h/m_e c$ emerges which may be considered as the size of the particle.

The electron obeys the kinematic laws and its electromagnetic interactions are perfectly described by Maxwell's equations and its extensions to quantum mechanics. Many models have been built to describe the nature of this particle. The simplest ones in the classical region substitute the point like charge by a sphere of radius r_e with surface charge e . The rest mass of the particle is then attributed to the electric field energy, the self-energy of the charge. One just defines then the classical electron radius, with twice the self-energy of such a charged sphere:

$$r_e = \frac{e^2}{4\pi\epsilon_0 \cdot m_e c^2} = 2.8 \cdot 10^{-15} [m] . \quad (6)$$

Such a model needs an artificial attractive force to compensate the electrostatic repulsion in the center [7].

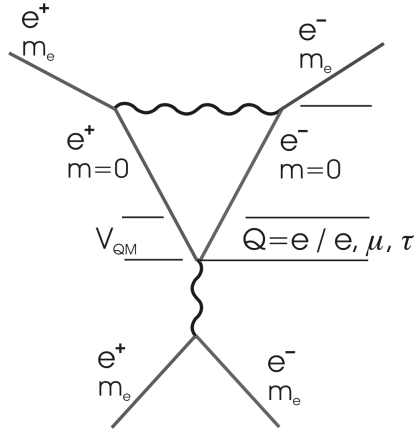


Fig. 3. In this picture an electron-positron pair with masses m_e is annihilated at high energy and creates a virtual massless charge pair. Inside the volume V_{QM} quantum electrodynamics decides that the charge Q will be the elementary charge e and either an e^- , μ^- , or a τ^- -pair will be created. Within about $t = h/m_e c^2 = 10^{-20}$ sec for an electron pair the mass will then be formed.

The next step is to put the charge on a circular orbit or on a spinning top to explain spin and magnetic moment [3] [4] [5]. Special assumptions have always been necessary to cover most of the properties of the particle.

Special relativity leads to discrepancies if one associates the mass to the field energy of a charged sphere: The momentum of a moving electron as well as the “kinetic energy” given by the magnetic field of its current yield both the same value for the mass. This is however bigger than that derived from the self-energy of the electric field [6].

The other approach to explain the electron structure comes from the wave mechanical side. It may be modeled by an oscillating charge distribution [7] or by the movement of toroidal magnetic flux loops [8]. Many more recent contributions follow this direction. They are based on a paper by Barut and Zanghi [9] in which a closed internal field moves with speed of light, the Zitterbewegung, on special tracks. They are able to adjust their models with the boundary conditions of the wave to yield the fixed angular momentum, the magnetic moment, the charge and the mass. The stability of the tracks have topological reasons. Knots in the trajectory e.g. should prevent from decay [10] [11].

One is meanwhile accustomed to the view that classical mechanics and wave mechanics describe two different worlds perfectly described by electrodynamics and quantum electrodynamics with its extensions. A wide gap between both exists which is not closed up to now by a satisfactory classical description.

The existing classical models deal with relativistic charges but disregard the generation of synchrotron radiation. Synchrotron radiation is dominant especially if one designs an electron by a circulating massless charge field which seems to be a promising concept.

It is the purpose of this paper to find out if the classical view can be extended by this picture to close the gap between classical electrodynamics and the wave description of the electron by considering the emission of synchrotron radiation.

The creation of massless charge fields e.g. by an annihilation of an electron-positron pair is visualized by the Feynman graph in Fig. 3. One expects that the high energy density at the interaction point leads immediately to quantum mechanical processes which generate the elementary charge e and decide the particle family such as electron, muon or tau. There is still time of the order of $h/m_e c^2 = 10^{-20}$ sec for the electron to generate its mass.

In this picture a massless charge field exists in the meantime. It moves with speed of light and may lead to a stable configuration if the path is bent e.g. by scattering processes or by electromagnetic background fields.

- First a massless charge field is considered which moves with speed of light on the most simple, a circular orbit to investigate its radiation. (Such orbits are possible in spherical radiation fields discussed below.)
- The synchrotron radiation of this charge is described by the inhomogeneous wave equation which is solved numerically in the near and far zone.
- The resulting properties give a first opportunity to compare these with the properties of the real electron.
- The solutions of the *homogeneous* equation describe how any radiation i.e. also the synchrotron radiation propagates in space. A special solution in spherical coordinates yields a background field which rotates in azimuthal direction.
- The electric field lines of the spherical background field are investigated. They are smooth and may lead to stable paths of the massless charge field.
- It will be shown that a finite total energy of the background field is possible which can be attributed to the radiation energy of the electron.
- The relation of the electromagnetic field energy and the mass are discussed.

II. THE SYNCHROTRON RADIATION OF THE CIRCULATING CHARGE

In the Feynman diagram in Fig. 3 it is assumed that a massless charge pair was created. It moves with speed of light $\beta = v/c = 1$ and will immediately be deflected from its path by radiation processes. The simplest assumption is that the charge fields move on circular paths in a central field deflected by radiation processes. Such a central field may exist as will be shown in sections III to V.

The synchrotron radiation of a charge is described by the solutions of the *inhomogeneous* wave equations for the electric potentials of the charge \vec{A} and Φ e.g. expressed in Cartesian coordinates [12]:

$$\begin{aligned} \Delta \vec{A} - \frac{1}{c^2} \frac{\partial^2 \vec{A}}{\partial t^2} &= -\mu_0 \vec{j}; \\ \Delta \Phi - \frac{1}{c^2} \frac{\partial^2 \Phi}{\partial t^2} &= -\frac{\rho}{\epsilon_0}. \end{aligned} \quad (7)$$

The solution of the *homogeneous* wave equation describe the propagation of the radiation ($\Phi = 0$ may be chosen):

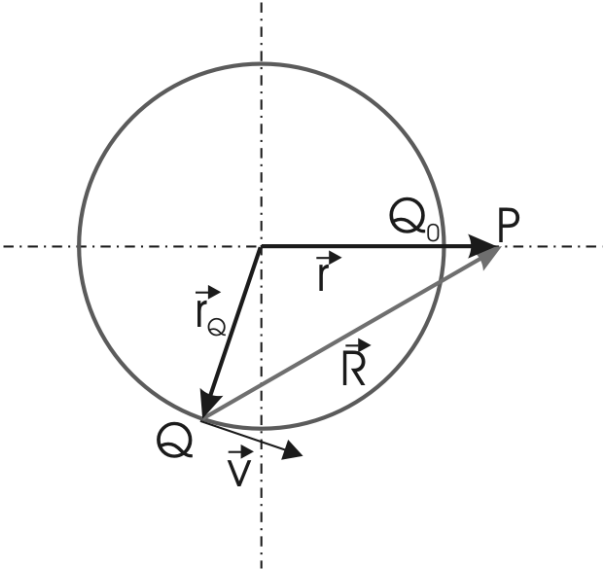


Fig. 4. An observer at position $P(\vec{r}, t)$ looks at the fields of a charge traveling on a circular orbit with velocity \vec{v} . He detects the fields which have been emitted at Q at an earlier time $t_Q - t$. For $|\vec{v}| = c$ the distance R equals to the length of the arc $(Q(t_Q), Q_0(t))$

$$\Delta \vec{A} - \frac{1}{c^2} \frac{\partial^2 \vec{A}}{\partial t^2} = 0. \quad (8)$$

This equation is discussed in section III.

Solutions of the *inhomogeneous* equations are the retarded Liénard-Wiechert potentials [12]

$$\Phi(\vec{r}, t, r_Q^-, t_Q) = \frac{e}{4\pi\epsilon_0} \frac{1}{R - \vec{R} \cdot \frac{\vec{v}}{c}} \quad (9)$$

$$\vec{A}(\vec{r}, t, r_Q^-, t_Q) = \frac{\mu_0 e}{4\pi} \frac{\vec{v}}{R - \vec{R} \cdot \frac{\vec{v}}{c}}. \quad (10)$$

An Observer $P(\vec{r}, t)$ receives the fields from the circulating charge Q from an earlier position $Q(r_Q^-, t_Q)$ sketched in Fig. 4. The vector \vec{R} is given by $\vec{R} = \vec{r} - r_Q(t_Q)$ and \vec{v} is the velocity of the charge at the emission point. If the charge reaches Q_0 at time t the length R is as long as the arc (Q, Q_0) for $\beta = 1$.

One computes the distance R between $P(r, \vartheta, \varphi, t)$ and the charge for each position of Q , φ_Q , $\vartheta_Q = \pi/2$ by

$$R^2 = r^2 + r_Q^2 - 2rr_Q \sin \vartheta \cos(\varphi - \varphi_Q), \quad (11)$$

with $\varphi_Q = \omega \cdot t_Q$, $t_Q = t - R/c$ and $\omega = \beta c/r_Q$ one gets $\varphi - \varphi_Q = \varphi - \omega t + \beta R/r_Q$. This is $\phi + \beta R/r_Q$, if one substitutes $\phi = \varphi - \omega t$. One obtains

$$\frac{R^2}{r_Q^2} = \frac{r^2}{r_Q^2} + 1 - 2 \frac{r}{r_Q} \cos(\phi + \beta \frac{R}{r_Q}). \quad (12)$$

The component of \vec{R} along the velocity \vec{v} is then given by

$$R_v = \vec{R} \cdot \vec{v} / v = r \sin(\phi + \beta \frac{R}{r_Q}). \quad (13)$$

The electric and magnetic fields are

$$\vec{\mathcal{E}} = -\vec{\nabla} \Phi - \frac{\partial \vec{A}}{\partial t}; \quad \vec{\mathcal{H}} = \frac{1}{\mu_0} \text{curl} \vec{A}. \quad (14)$$

They lead to the equations [12]

$$\vec{\mathcal{E}} = \frac{e}{4\pi\epsilon_0} \left[\begin{array}{l} (1 - \beta^2) \frac{\vec{R} - R \frac{\vec{v}}{c}}{(R - \beta R_v)^3} \\ - \frac{\vec{R} \times ((\vec{R} - R \frac{\vec{v}}{c}) \times \dot{\vec{v}})}{c^2 (R - \beta R_v)^3} \end{array} \right] \quad (15)$$

$$\vec{\mathcal{H}} = \epsilon_0 c \cdot \frac{1}{R} [\vec{R} \times \vec{\mathcal{E}}]. \quad (16)$$

The first term within the brackets of equation (15) describes the field connected to the moving charge and the second term which contains the acceleration yields the radiation.

The denominators of both parts become zero for $\beta = 1$ if \vec{R} is tangential to the orbit. For a circular track in the horizontal plane ($\vartheta = \pi/2$) all singularities are located on this plane at $R = \sqrt{(r/r_Q)^2 - 1}$ i.e. at $r > r_Q$. Thus a small region around this singularity is dominated by quantum mechanical phenomena because of the huge energies. This region at $\vartheta = \pi/2$ has to be excluded in classical considerations.

It is interesting to note that the first term vanishes outside the quantum mechanical volume for $\beta = 1$. It represents an uncharged object which can only consist of electromagnetic waves. Only the second part describes the properties of the charge and its synchrotron radiation as well.

The evaluation of the radiation parts of the equations (15) and (16) in spherical coordinates yield the spherical components of the fields:

$$\text{with} \quad f_E = \frac{e}{4\pi\epsilon_0} \frac{\beta^2}{4rr_Q^2 (R - \beta R_v)^3} \quad (17)$$

$$\mathcal{E}_r = -f_E \left[\begin{array}{l} [(R + r_Q)^2 - r^2] \cdot \\ [(R - r_Q)^2 - r^2] \\ + 4\beta r_Q^2 R R_v \end{array} \right] \quad (18)$$

$$\mathcal{E}_\vartheta = -f_E \frac{\cos \vartheta}{\sin \vartheta} \left[\begin{array}{l} 4\beta r_Q^2 R R_v - r^4 \\ + (R^2 - r_Q^2)^2 \end{array} \right] \quad (19)$$

$$\mathcal{E}_\varphi = f_E \frac{2r_Q}{\sin \vartheta} \left[\begin{array}{l} \beta R [R^2 - r_Q^2] \\ + r^2 (1 - 2 \cos \vartheta^2) \\ - R_v (+R^2 - r_Q^2 + r^2) \end{array} \right] \quad (20)$$

$$\text{and with} \quad f_H = \frac{e c}{4\pi} \frac{\beta^2}{2r_Q (R - \beta R_v)^3} \quad (21)$$

$$\mathcal{H}_r = f_H \cos \vartheta \beta (R^2 - r^2 + r_Q^2) \quad (22)$$

$$\mathcal{H}_\vartheta = f_H \frac{1}{\sin \vartheta} \left[\begin{array}{l} \beta (R^2 + r^2 + r_Q^2) \cos \vartheta^2 \\ - 2R(\beta R - R_v) \end{array} \right] \quad (23)$$

$$\mathcal{H}_\varphi = f_H \frac{\cos \vartheta}{\sin \vartheta} \left[\begin{array}{l} r_Q^2 (2R_v - R) \\ + R(R^2 - r^2) \end{array} \right] \quad (24)$$

With these fields the following results are obtained.

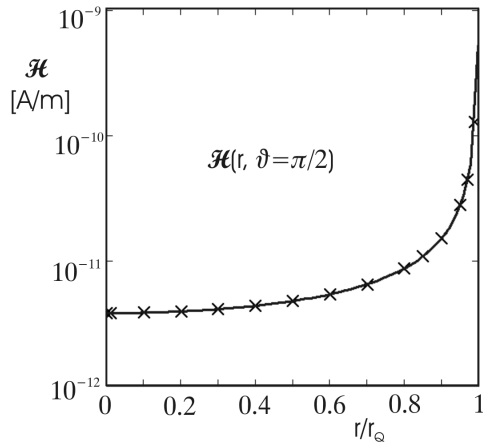


Fig. 5. The size of the magnetic field of a charge e circulating at a radius r_Q with speed of light is shown as full line as a function of r . It was computed from the current according Biot-Savart's law. The mean magnetic field of eq.(23) at $\vartheta = \pi/2$ inside the circle are inserted as x-symbols and are on top of the curve.

A. Comparison with Experimental Results

1) *The magnetic moment and the extension of the electron:* A classical circulating charge is expected to generate a magnetic moment. Here the charge is a massless charge field which travels on a circular path as the simplest assumption. The mean magnetic field of the circulating charge field is compared in Fig. 5 with the magnetic field of a classical circular current $I = ec/2\pi r_Q$ with radius r_Q . The magnetic fields are determined in the mid plane ($\vartheta = \pi/2$) for $r < r_Q$. The crosses from the charge field are on top of the curve from the current. Both descriptions are equivalent. From the experimental value of the magnetic moment $\mu_e = 1.00116(e\hbar/2m_e)$ and $\mu = Ir_Q^2\pi$ the radius of the circular path in the present model results in

$$r_Q = 2\mu_e/ec = 3.87 \cdot 10^{-13} [m] \quad (25)$$

which determines the size of the electron. The inverse we need later is calculated to

$$k = 2.59 \cdot 10^{12} [m^{-1}], \quad (26)$$

and the fundamental frequency is

$$\omega = c/r_Q = 7.75 \cdot 10^{20} [s^{-1}]. \quad (27)$$

The length of the circular path can be associated to a wavelength belonging to the fundamental frequency ω

$$\lambda_e = 2\pi r_Q = 1.00116 \cdot h/m_e c [m]. \quad (28)$$

This is just the Compton wavelength of the electron.

Quantum mechanics predicts the energy according to

$$E = \hbar\omega = 8.18 \cdot 10^{-14} [J], \quad (29)$$

which is consistent with the electron mass of $m_e c^2 = 8.187 \cdot 10^{-14} [J]$.

From the reproduction of the experimental values with these simple assumptions one must conclude that higher harmonics are negligible.

2) *The electric field of the radiation part:* It should be emphasized again that there is no static electric field connected to the charge moving with $\beta = 1$. The only electric field is that of the radiating part. It should be equal to the Coulomb field when averaged over the surface of a sphere surrounding the charge.

The electric field of a charge e computed by Coulomb's law is plotted as full line in Fig. 6 as a function of the distance r/r_Q . The +-signs on top of the curve display the radial components of the field of eq.(18) at the respective distances. The field was averaged over the surface of the sphere with radius r over the intervals $[-\pi \leq \Delta\phi \leq -10^{-4}]$, $[10^{-4} \leq \Delta\phi \leq \pi]$ with $\Delta\phi$ the deviation of ϕ from the singularity, and over $[0.001 \leq \vartheta \leq 0.824\pi/2]$ (and symmetric to the mid plane).

The field is not spherical symmetric like in Coulomb's law. The field now averaged over $\Delta\phi$ shown in Fig. 7 as a function of ϑ dominates close to the mid plane.

B. The Poynting vector

Both the electric and the magnetic field of the synchrotron radiation are combined in the Poynting Vector, which yields the power density of the radiation

$$\vec{S} = \vec{E} \times \vec{H}. \quad (30)$$

The Poynting vector close to the circulating charge is directed into a narrow cone in forward direction [12]. It has a strong azimuthal component which is responsible for the angular momentum of the object.

The azimuthal component is transformed in the far region into a radial component and may be used to determine the total radiated power. This will be discussed first.

1) *The radial component of the Poynting vector in the far zone:* The radial component of the synchrotron radiation dominates in the region far from the circulating charge. Approximations in this region allow for analytic evaluations which is normally done by Fourier decomposition [15] [16] [17]. In the present paper the Poynting vector is evaluated without these approximations by numerical methods.

The radial component of the Poynting vector S_r at $r = 10^5 r_Q$ is plotted in Fig. 8 in the interval $\Delta\phi = [-\pi, \pi]$ around its singularity discussed with eqs. (18) - (24). Curves for different ϑ -values are shown. S_r increases exponentially at small distances $\Delta\phi$ from the singularity where one expects dominating quantum electrodynamic properties. This strong increase at small distances from the singularity at $\vartheta = \pi/2$ is also seen in Fig. 10 in the power P_r radiated through the surface of the sphere with radius $r = 10^5 r_Q$ when the integration interval in ϑ ($0, \vartheta_{max}$) approaches $\vartheta = \pi/2$.

The total radial radiation power as a function of r is plotted in Fig. 11. The power saturates at large distances when S_φ transforms more and more into S_r .

The energy loss of the permanently circulating charge seems to be in contradiction to a stable electron model. This problem will be addressed in sections III and IV.

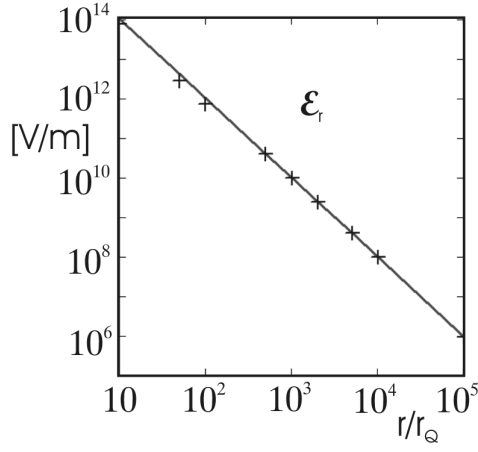


Fig. 6. Electric field \mathcal{E}_r of a point charge $Q = +e$ according to Coulomb's law as a function of the distance r/r_Q . The +-signs on top of the curve represent the radial field given by eq.(18) averaged over the surface of the respective spheres.

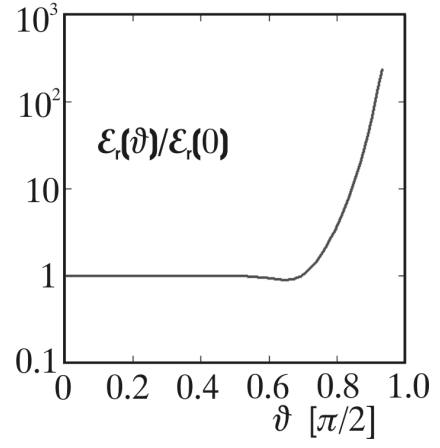


Fig. 7. Radial electric field given by eq.(18) averaged over ϕ , the azimuthal position of the observer, as a function of the polar angle ϑ .

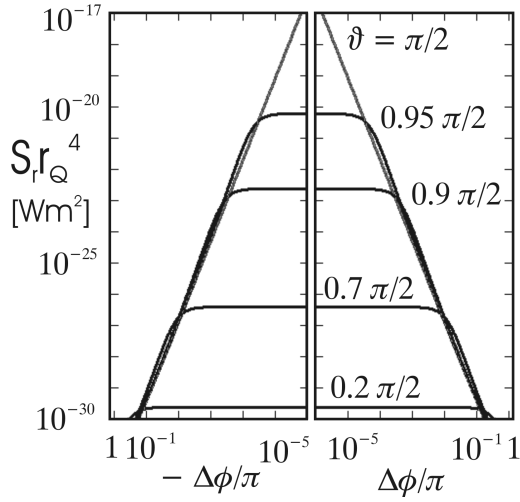


Fig. 8. Radial component of the Poynting vector S_r at $r = 10^5 r_Q$ for different ϑ values as function of the azimuthal deviation from the maximum. The plot is in a double logarithmic scale to expand the singularity of eq. (30).

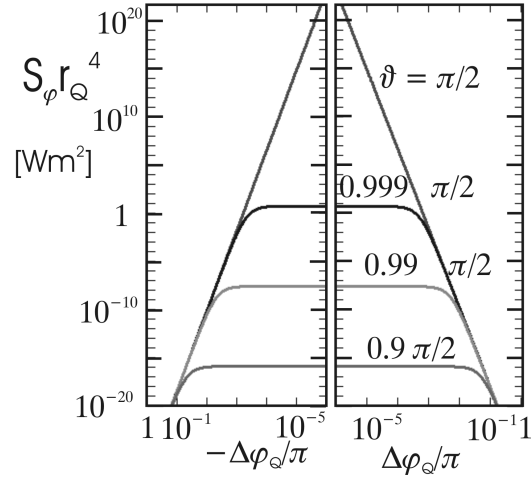


Fig. 9. Azimuthal component of the Poynting vector S_φ for the second last circulation as function of the azimuthal deviation from the maximum. Different ϑ -values were chosen.

2) *The azimuthal component of the Poynting vector:* The azimuthal component of the Poynting vector is better viewed from the responsible position of the charge φ_Q . The fields from the charges moving in the range of $-2\pi \leq \varphi_Q \leq 0$ reach observers $P(r, \vartheta = \pi/2, \varphi = 0)$ at radii between $r = (1 + 2\pi)r_Q$ and r_Q , former circulations between $-n2\pi \leq \varphi_Q \leq -(n-1)2\pi$ arrive between $r = (1 + n2\pi)r_Q$ and $r = (1 + (n-1)2\pi)r_Q$ respectively. These values change slightly for observers at different polar angles ϑ . A smaller range of the first circulation is responsible for the fields of the inner volume.

The azimuthal component of the Poynting vector generated e.g. by the second last circulation $n = 2$ from $r = (1 + 2\pi)r_Q$ to $r = (1 + 4\pi)r_Q$ is shown in Fig. 9 for various ϑ -values as a function of φ_Q . The horizontal axes is centered at the forward maximum where R is tangential to the circular track.

3) *The angular momentum of the synchrotron radiation:* The azimuthal component of the Poynting vector is responsible for an angular momentum around the vertical axis of the object. It is computed by

$$L = \frac{1}{c^2} \int S_\varphi(r, \vartheta, \phi) r^3 dr \sin^2 \vartheta d\vartheta d\phi. \quad (31)$$

Since the field of the charge at r_Q reaches an observer $P(r, \vartheta, \phi)$ only at a specific r -value r will be substituted by $r = r(\varphi_Q)$, dr by $dr/d\varphi_Q$ and the integration is performed over one circulation of the charge.

The path of the charge field is further on assumed to be circular. The angular moment in units of \hbar for the last but one circulation is plotted in Fig. 12. It is strongly dependent on the interval of integration in φ_Q and ϑ because of the presence of the singularity. Curves with different excluded regions of $\pm\Delta\varphi_Q$ around the centered singularity are plotted

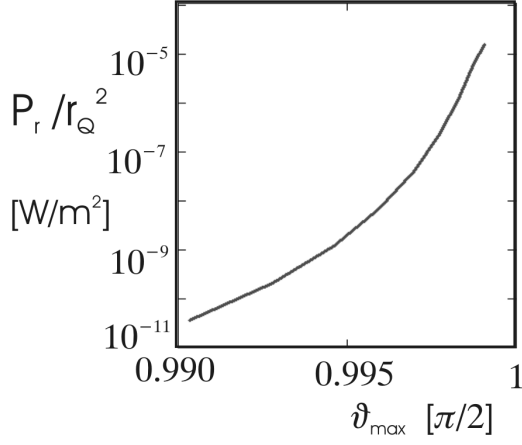


Fig. 10. Emitted radiation power in radial direction P_r at $r = 10^5 r_Q$ integrated between $\vartheta = 0.01$ and ϑ_{max} .

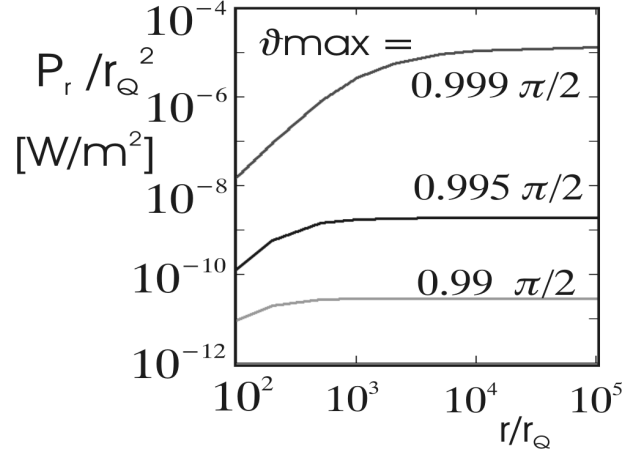


Fig. 11. Emitted radiation power in radial direction P_r integrated between $\vartheta = 0.01$ and ϑ_{max} as function of the relative distance r/r_Q .

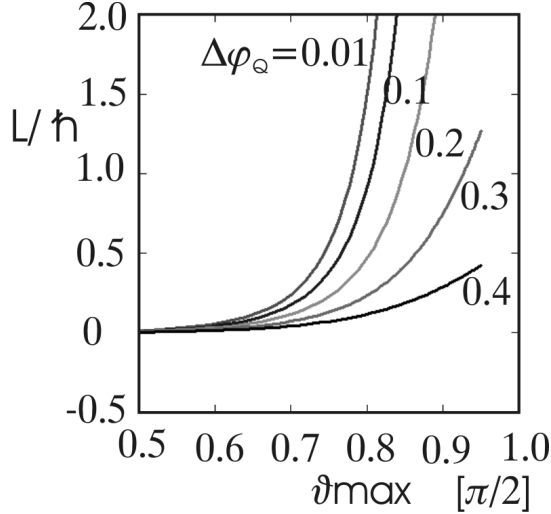


Fig. 12. Angular momentum of the synchrotron radiation in units of \hbar when integrated from $\vartheta = 0$ to ϑ_{max} (and symmetric to the mid plane). Different regions $\pm\Delta\varphi_Q$ were cut out around the singularity.

as a function of ϑ_{max} the upper limit of the integration interval. The values symmetric to the mid plane have been added. The present circulation gives slightly different values, but averages out. The angular moments of former circulations which feed higher distances are almost identical.

One sees that it is possible by reasonable cuts $\Delta\varphi_Q$ and ϑ_{max} to receive angular momenta in the right order of magnitude.

III. THE SOLUTION OF THE HOMOGENEOUS DIFFERENTIAL EQUATION

The next step is to solve the homogeneous differential equation, the wave equation (8). It describes the propagation of any radiation in space. Usually it is solved in Cartesian coordinates in which the components separate and the subsequent transformation to cylindrical components allows for the investigation of multipole properties [18]. One is

interested here in *spherical* components as obtained with the inhomogeneous equations in section II.

The relation

$$\vec{curl} \vec{curl}(\vec{A}) = \nabla(\nabla \vec{A}) - \Delta \vec{A} \quad (32)$$

which is used with Cartesian coordinates is not valid in a spherical coordinate system. The wave equation in vacuum for the vector field \vec{A} in spherical coordinates and with spherical components has therefore the form

$$\vec{curl} \vec{curl}(\vec{A}) - \frac{1}{c^2} \frac{\partial^2 \vec{A}}{\partial t^2} = 0 \quad (33)$$

The same equation is also valid for \vec{H} and \vec{E} .

If one writes \vec{A} as a product in spherical coordinates, e.g. for the space component

$$A_r = \mathcal{R}_r(x) \cdot \Theta_r(\vartheta) \cdot \Phi_r(\varphi) \cdot \mathcal{T}(t) \quad (34)$$

and with

$$\begin{aligned} \mathcal{T}(t) &= e^{\pm i\omega t} \quad \text{and} \\ \Phi(\varphi) &= e^{\pm im\varphi}, \quad k = \omega/c, \quad kr = x \end{aligned} \quad (35)$$

the wave equation separates in the coordinates, and one obtains 2 solutions which are dependent via Maxwell's equations, if attributed to \vec{H} and \vec{E} respectively. Special solutions, periodic in φ , finite and smooth at the origin with waves in φ -direction have standing waves in r and ϑ :

$$\begin{aligned} \mathcal{H}_r &= 0 \\ \mathcal{H}_\vartheta &= -C_k C_m eck^2 (2m-1) P_{m-1}^{m-1}(\vartheta) \cdot j_m(x) \cos(m\varphi - kct) \end{aligned} \quad (36)$$

$$\begin{aligned} \mathcal{H}_\varphi &= C_k C_m eck^2 P_m^{m-1}(\vartheta) \cdot j_m(x) \sin(m\varphi - kct) \end{aligned} \quad (37)$$

$$\mathcal{E}_r = -\frac{C_k C_m e k^2}{\varepsilon_0} (m+1) P_m^m(\vartheta) \cdot \frac{j_m(x)}{x} \cos(m\varphi - kct) \quad (38)$$

$$\mathcal{E}_\vartheta = -\frac{C_k C_m e k^2}{\varepsilon_0} \frac{P_m^{m-1}(\vartheta)}{2m+1} \cdot [(m+1)j_{m-1}(x) - m j_{m+1}(x)] \cdot \cos(m\varphi - kct) \quad (39)$$

$$\mathcal{E}_\varphi = \frac{C_k C_m e k^2}{\varepsilon_0} \frac{2m-1}{2m+1} P_m^{m-1}(\vartheta) \cdot [(m+1)j_{m-1}(x) - m j_{m+1}(x)] \cdot \sin(m\varphi - kct) \quad (40)$$

The $P_n^m(\vartheta)$ are the Associated Legendre Functions, $j_n(x)$ are Spherical Bessel Functions [13] [14], and the factors in front are chosen to give the right dimensions. C_k and C_m are normalization constants. The wave functions are unambiguous for $m = 1, 2, 3, \dots$, and the separation constant k determines the size of the whole object. More details may be found in appendix A.

The general solution of this central wave is then a sum over all the harmonics m and over the wave numbers k , with the coefficients C_m and C_k , chosen to satisfy the boundary conditions. If the central wave should describe the propagation of the synchrotron radiation of a charge on the special circle assumed in chapter II then k is already fixed by eq.(26).

The Bessel functions subdivide the fields into shells with alternating field directions from one to the next. It is shown in Fig. 13(a) for $j_1(x)$, and the logarithmic plot in Fig. 13(b) demonstrate the decrease of the amplitude like $1/x$ at high x . This is true for all n . Only \mathcal{E}_r decreases with $1/x^2$.

A sketch of the fields \vec{H} and \vec{E} for $m = 1$ for the innermost shells is displayed in Fig. 14.

IV. THE SYNCHROTRON RADIATION AND THE CENTRAL WAVE.

The eqs.(36) and (38) can describe the propagation of any radiation in space: the strong radiation generated in the annihilation process as well as the synchrotron radiation of the circulating charge. If the electron would exist as a stable radiation object the current of the charge and the radiation would influence each other: the emission of synchrotron radiation would generate a permanent central electromagnetic background field which on the other hand would be absorbed again by the charge and compensates the energy loss.

To simplify the discussion it is still assumed that the charge moves on a circular track and the scattering by the radiation processes is neglected. For the central wave also the lowest mode $m = 1$ is considered for the moment.

The power of the synchrotron radiation in φ -direction and the azimuthal power of the central wave must be the same in a complete solution and are compared in Fig. 15. The horizontal axis displays the distance x which is equivalent to r/r_Q . The synchrotron radiation is integrated up to $\vartheta = 0.9\pi/2$ and the narrow peaks of the synchrotron radiation demonstrate the large content of higher harmonics. The Fourier analysis of the azimuthal component of the Poynting vector of Fig. 9 with

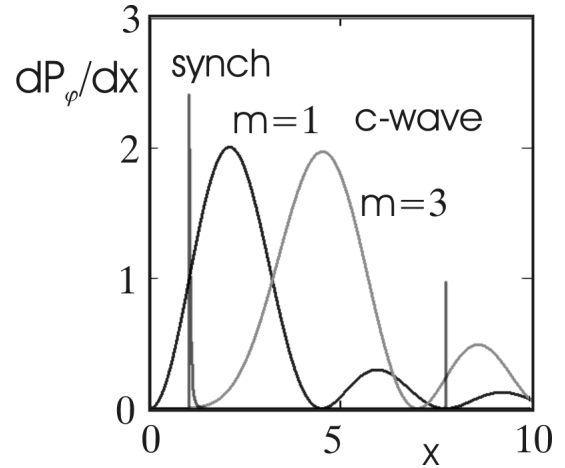


Fig. 15. Azimuthal power distribution dP_φ/dx of the synchrotron radiation and of the central wave with $m = 1$ and $m = 3$ as a function of x ($\equiv r/r_Q$). The functions are arbitrarily scaled.

$\vartheta = 0.9\pi/2$ yields e.g. a frequency distribution with a width at half height of about 100 times the fundamental frequency.

The overlap of the radiation with the central wave is best with the fundamental frequency ($m = 1$). The higher harmonics of the central background with higher m -values start all at higher x . This is a hint that the synchrotron radiation is described with waves close to the fundamental frequency.

The standing wave in x -direction is governed by the slow decrease of the Bessel functions. This contradicts the finite angular momentum and the finite total energy of a finite radiation cloud if the central wave should describe the radiation content of a real electron.

The angular momentum of the circulating wave integrated up to x_{max} is displayed in Fig. 16. The scale of the angular momentum is arbitrary because the coefficients C_k and C_m for $m = 1$ were just chosen to be 1. The angular momentum increases with x_{max} to infinity for a solution when $m = 1$ only is used. A Fourier like expansion in φ is needed to yield a finite result. Already the addition of a counter rotating contribution with $m = 3$ and the coefficients $C_3/C_1 = 0.056$ leads to a constant but still oscillating result. An inclusion of terms with $m = 2$ and $m = 4$ had a minor effect. Higher terms could not be tested because of the limited accuracy of the computing program.

The electric and the magnetic energy of the central wave sum up to a constant energy density dE/dx respective to x as displayed in Fig. 17. This would lead to an infinite total energy.

Again an expansion is needed to obtain a finite value. The functions (36) etc. may be considered as members of a Fourier-Bessel expansion [19] [20]:

$$f(r) = \sum_i A_i j_m(k_i r) = \sum_i B_i j_m(\lambda_i x) \quad (41)$$

This may obviously be applied at $t = 0$. If e.g. for $m = 1$ $j_1(x)$ in $\mathcal{H}_\theta(x)$ is substituted by the truncated function shown in Fig. 18 and expanded in the region $0 \leq x \leq 40$ the sum contains 12 terms. But this replacement is not valid in

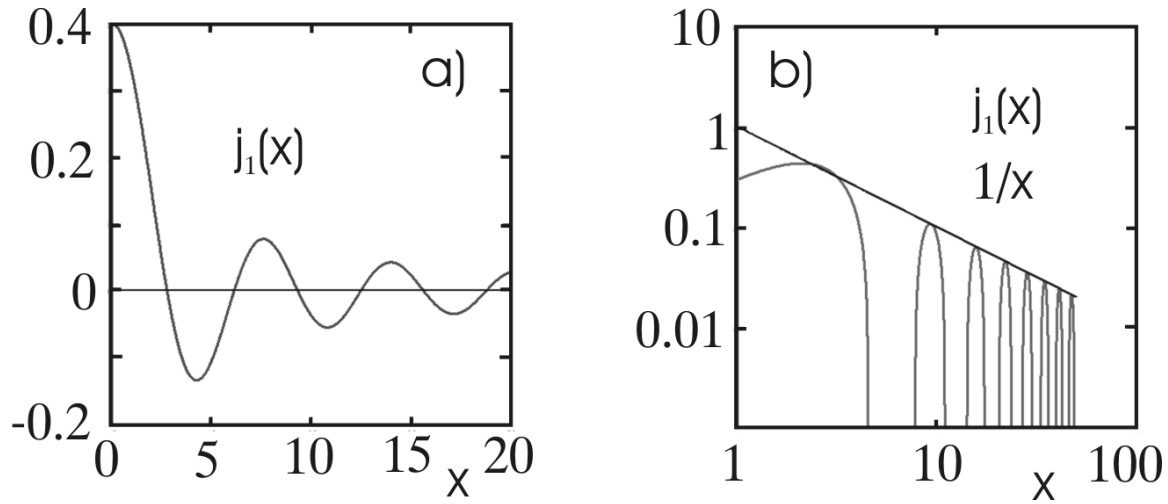


Fig. 13. The space parts for $\mathcal{H}_{\theta,\varphi}$, \mathcal{E}_r and \mathcal{E}_{φ} given by the respective $j_n(x)$ are shown for $m = 1$ (a) in linear and (b) in logarithmic plots. The amplitudes decrease with $1/x$.

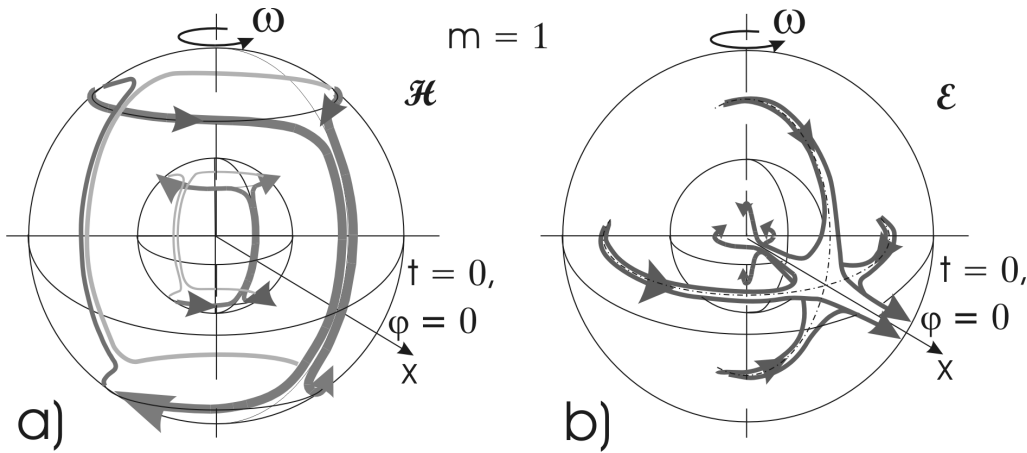


Fig. 14. Sketch of the \mathcal{H} - and the \mathcal{E} -field for $m = 1$. The spheres in a) on which \mathcal{H} is located are also shown in b).

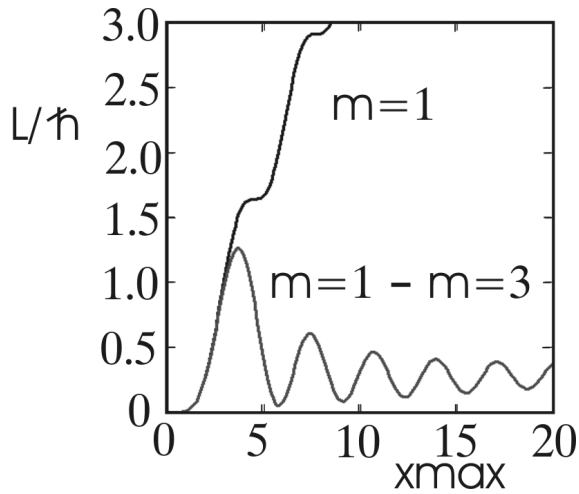


Fig. 16. Angular momentum of the central wave in units of \hbar integrated up to x_{\max} . The label "m=1" assigns the contribution of the special solution with $m = 1$ only. In "m-1 - m-3" a special solution with $m = 3$ is subtracted. $C_1 = 1$ was used.

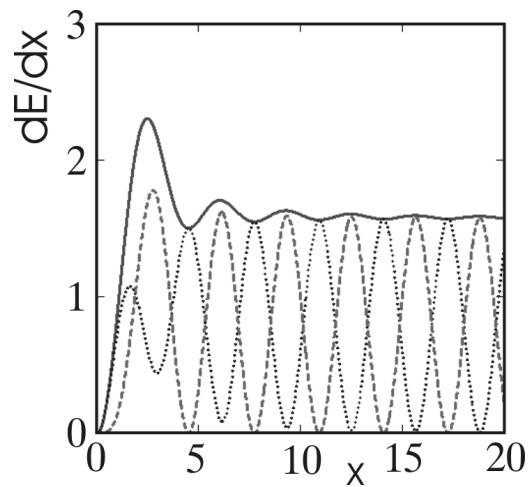


Fig. 17. Energy density dE/dx of the electric (\cdots), and the magnetic field ($---$) of the central wave, and the sum of both (solid line) as a function of x (vertical axes unscaled).

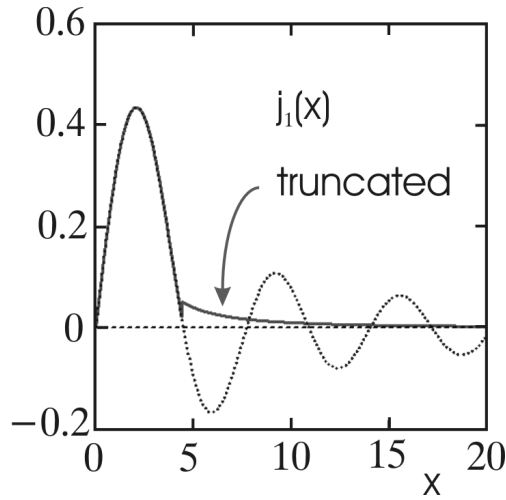


Fig. 18. $j_1(x)$ and the truncated function which were expanded in a Fourier-Bessel series.

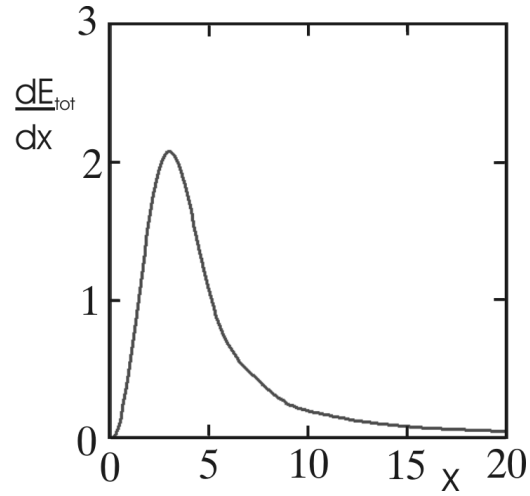


Fig. 19. Total energy density dE/dx after the replacement of k in the central wave by $\lambda_i k$ and summed with coefficients obtained by the Fourier-Bessel expansion obtained by the truncation like in Fig. 18 .

general for the whole set of wave functions. These equations are only satisfied if all occurrences of k are replaced by $\lambda_i k$. Nevertheless one finds that the expansion leads also to a good approximation for the wave functions which is proven by the finite total energy shown in Fig. 19.

V. THE MASSLESS CHARGE IN THE CENTRAL WAVE

It has been shown that the synchrotron radiation of a relativistic circulating charge generates a circulating electromagnetic background field. The question is if on the other hand the background field guides the charge on a circular path and both form an object even a finite one which can be called an electron.

The simplest configurations have been assumed up to now: a charge moving on a circular track and a background field with $m = 1$ and a single k -value. The discussions in section IV already showed that a superposition of waves should be present. It will be shown in this section how a charge may move in such a central background field.

A charge moving in the central wave with velocity v sees an effective electric field ($\vec{E} + \mu_0 \vec{v} \times \vec{H}$) which forces the charge to follow the field lines. This is possible by emitting radiation to balance the momentum, and the statistical emission and absorption of radiation will result in deviations.

To trace the field lines a massless charge probe which moves with speed of light and which just follows the effective field was inserted. Its track under different conditions was recorded.

The various harmonics differ in the symmetry regarding φ which results in different phase velocities. This velocity is c at the radius $x = m$.

Field lines have been traced for waves with $m = 1$, $m = 2$, and $m = 3$ and for many starting points. A smooth field line has always been found for each condition in the mid plane $\vartheta = \pi/2$ and the field lines stayed in the mid plane if started there.

Four special field lines in the mid plane ($\vartheta = \pi/2$) seen by a charge with $|\vec{v}| = c$ are drawn for $m = 1$ in Fig. 20. The axes are the Cartesian coordinates (ξ, ψ) of x . There is the circular field line with a radius of $x = m = 1$, the next one oscillates towards the center, and the next oscillates around $x = 2$. The one oscillating around $x = 3$ shows counter rotating loops. The small loops become more and more flat for field lines further outward. The field lines can cross each other because they are functions of the coordinates and of the velocities as well.

The field lines for $m = 2$ and higher are similar but are modified according to the different symmetry. A probe with opposite charge moves just at the same distance but opposite to the origin.

Smooth field lines have also been obtained outside the mid plane. They are similar to the ones already discussed but oscillate vertically. The field line e.g. corresponding to the circular one in Fig. 20 is shown in Fig. 21(a) in a top view and in (b) in a side view as function of φ . The line starts horizontally at the Cartesian coordinates of x $(\xi, \psi, \zeta) = (0, -0.98, 0.41)$ and oscillates down to $\zeta = 0.23$. For comparison: field lines in the mid plane show oscillations in ζ of only 10^{-16} given by the numerical accuracy.

Field lines below the mid plane are vertically mirror symmetric.

One further example which corresponds to the innermost field line in Fig. 20 is shown in Fig. 22. The line starts horizontally here at $(\xi, \psi, \zeta) = (0, -1.3, 1.3)$. A toroid is also drawn into the top view for better visualization.

4) *Summation over harmonics and wave number* : The pictures in the previous section show that field lines with different shape already exist in a wave with constant k and $m = 1$. A charge in this field will therefore also generate synchrotron radiation of higher harmonics. On the other hand higher harmonics are also necessary if the total angular momentum of the system should be finite and a superposition

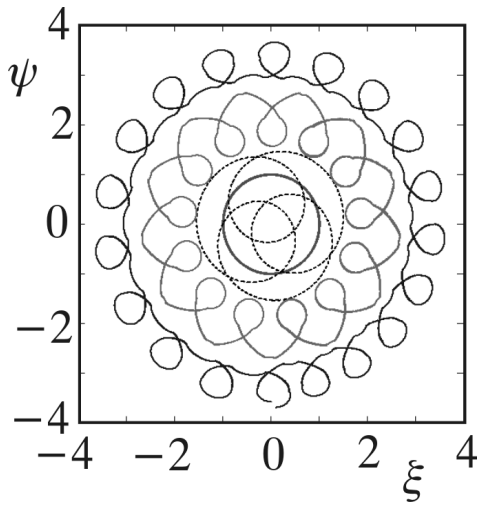


Fig. 20. Four selected closed effective electric field lines in the central wave with $m = 1$ seen by a charge moving with $|\vec{v}| = c$. The circular one has a radius of $x = 1$. The innermost oscillates towards the center, one oscillates around $x = 2$, and the outer one at $x = 3$ shows counter rotating loops. Shown is the mid plane $\vartheta = \pi/2$ in Cartesian coordinates of $x (\xi, \psi)$.

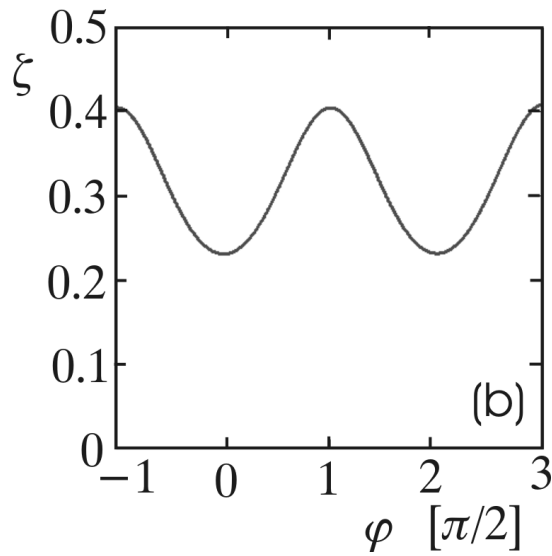
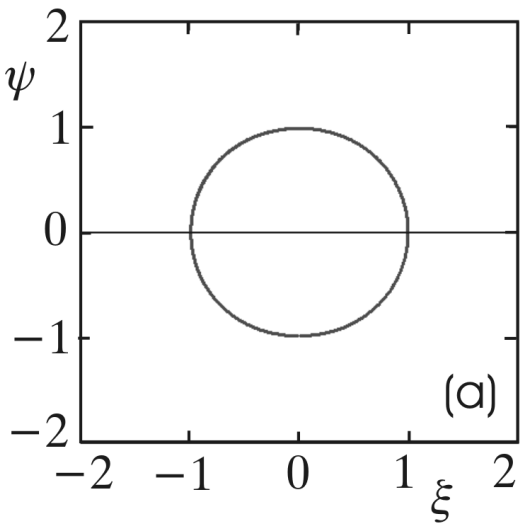


Fig. 21. Effective field line drawn by a massless test charge in the central wave with $m = 1$ above the mid plane. The line starts horizontally at the Cartesian coordinates $(\xi, \psi, \zeta) = (0, -0.98, 0.41)$. Fig.(a) shows the line in the top view, and Fig.(b) displays the vertical oscillation as a function of φ . Field lines below the mid plane are vertically mirror symmetric.

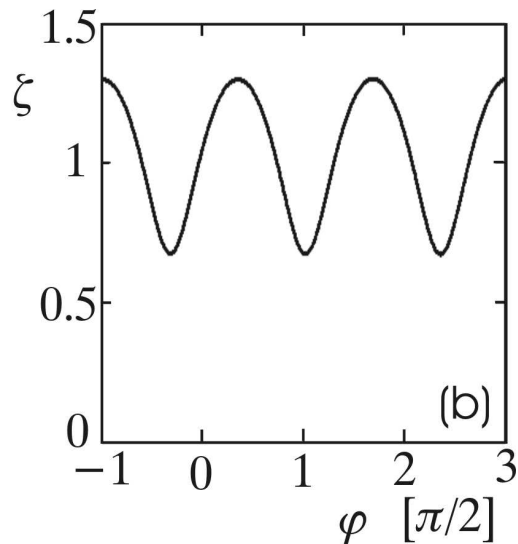
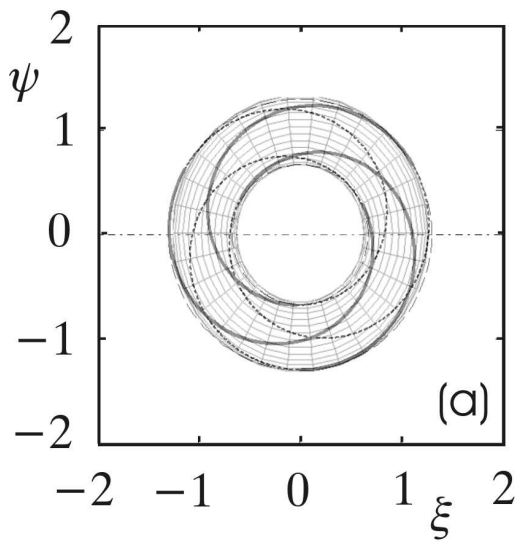


Fig. 22. Effective field line above the mid plane corresponding to the innermost field line of Fig. 20. It starts horizontally at $(\xi, \psi, \zeta) = (0, -1.3, 1.3)$. A toroid is inserted in the top view for better visualization.

with different wave numbers $k_i = \lambda_i k$ is necessary for a finite energy as discussed in section IV.

The field lines in a wave with $m = 1$ and $m = 3$ which lead to a finite angular momentum (Fig. 16) are unchanged below $x = 2$ but are deformed at higher distances from the center but they are all still smooth.

Field lines in a wave described by the example of a Fourier-Bessel expansion in Fig. 18 are also still smooth but radially oscillating.

It is the description of the synchrotron radiation by the central wave with finite solutions which will finally select the proper superposition.

VI. ON THE MASS OF THE ELECTRON

The electric field of a moving electron transports energy as well as momentum. The energy of the rest mass $m_e c^2$ is generally assumed to equal the self-energy of a suitable charge distribution. The kinetic energy of a moving charge, on the other hand, yields different mass energies via the momentum calculated with the Poynting vector and via the energy of the magnetic field of the current. This is in contradiction to special relativity [6].

One may expect that under Lorentz transformation e.g. in the x_1 -direction the energy transforms like $\bar{E} = \gamma E$ and the momentum like $(\bar{p}_1, \bar{p}_2, \bar{p}_3) = (\beta\gamma p_1, p_2, p_3)$ and $\bar{E}^2 - (\bar{p}c)^2 = E^2 - (pc)^2 = (mc^2)^2$ should yield the mass of the object. This is not true in general because energy and momentum of the field don't form a 4-vector. They belong to an energy-momentum tensor $T_{\mu\nu}$ [21] [22] [23]. With

$$\begin{aligned} T_{00} &= \rho^E = \frac{\varepsilon_0}{2} \bar{\mathcal{E}}^2 + \frac{\mu_0}{2} \bar{\mathcal{H}}^2; \\ T_{0i} &= -\rho_{0i}^P c = -S_i / c; \\ T_{ik} &= \varepsilon_0 \left(\frac{1}{2} \bar{\mathcal{E}}^2 \delta_{ik} - \mathcal{E}_i \mathcal{E}_k \right) \\ &\quad + \mu_0 \left(\frac{1}{2} \bar{\mathcal{H}}^2 \delta_{ik} - \mathcal{H}_i \mathcal{H}_k \right); \\ &\quad i, k = 1 \dots 3, \text{ and } T_{\mu\nu} = T_{\nu\mu} \end{aligned} \quad (42)$$

ρ^E, ρ_{0i}^P are the energy and momentum densities of the field, \vec{S} the Poynting vector, and T_{ik} Maxwell's tension tensor. The trace of the tensor vanishes in the rest system of the fields.

Lorentz transformation yields then the energy and momentum of a conventional charge moving with velocity $v/c = \beta$

$$\begin{aligned} E^\beta &= \int \rho^{E\beta} d^3x^\beta \\ &= \frac{1}{\gamma} \int (\gamma^2 T_{00} + (\gamma^2 - 1) T_{11}) d^3x, \\ p_1^\beta c &= \int \rho_1^{P\beta} d^3x^\beta \\ &= -\beta\gamma \int (T_{00} + T_{11}) d^3x, \\ p_{2,3}^\beta &= \int \rho_{2,3}^{P\beta} d^3x^\beta \\ &= -\beta \int (T_{12,3}) d^3x = 0, \end{aligned} \quad (43)$$

and for the rest mass from the field squared

$$\begin{aligned} E^{\beta^2} - \vec{p}^{\beta^2} c^2 & \\ &= \gamma^2 \left[\int (T_{00} + \beta^2 T_{11}) d^3x \right]^2 \\ &\quad - \beta^2 \gamma^2 \left[\int (T_{00} + T_{11}) d^3x \right]^2. \end{aligned} \quad (44)$$

Variables without the superscript β indicate that they are in the rest frame.

Neither the field energy nor its momentum show the proper dependence on γ and the rest mass is not constant. The reason is that with this concept one has to introduce a charge distribution at the origin of the electron to avoid the singularity of Coulomb's law [23]. Inner forces result which have to be somehow compensated. One must require $T_{11} = 0$ if eq.(44) should be valid at any particle speed.

The situation in the present model is different: there exists a charged radiation bucket which moves with $\beta = 1$. The field energies are again the self energies with the singularity cut out. If one takes a differential section of the circular path where the charge moves in the 1-direction eq.(44) becomes now

$$\begin{aligned} E^{\beta^2} - \vec{p}^{\beta^2} c^2 &= \gamma^2 \left[\int (T_{00} + T_{11}) d^3x \right]^2 \\ &\quad - \beta^2 \gamma^2 \left[\int (T_{00} + T_{11}) d^3x \right]^2 \\ &= \left[\int (T_{00} + T_{11}) d^3x \right]^2. \end{aligned} \quad (45)$$

This is constant and may be defined as the mass energy of the charge $m_q c^2$.

$$m_q c^2 = \frac{2}{3} \varepsilon_0 \int \bar{\mathcal{E}}^2 d^3x \quad (46)$$

In addition there is the energy of the standing wave of the central wave background and of the quantum mechanic center $m_w c^2$. Both add then to the total mass energy of the electron

$$m_e c^2 = m_q c^2 + m_w c^2. \quad (47)$$

VII. CONCLUSION

The presented investigations suggest that the classical electron can be described by a circulating massless charge field.

The comparison with the experimental properties of the electron show that already a movement on a circular track results in a good consistency. The radius of the circulation results from the experimental value of the magnetic moment and is obtained to $r_Q = 3.81 \cdot 10^{-13} [m]$. It represents also the size of the object.

The values for the circulation frequency and the Compton wavelength follow directly, and with Planck's constant \hbar the mass of the electron is reproduced.

A small volume around the singularity of the charge field is required in which strong radiation processes lead to quantum mechanical effects. This volume has to be cut out in the present classical considerations.

The circulating charge emits synchrotron radiation and when moving with speed of light it is totally embedded in this radiation. The static field around the quantum mechanical volume vanishes and this part becomes neutral.

The angular momentum L/\hbar of the synchrotron radiation of this charge moving on a circle with radius r_Q yields reasonable values of the order of 1 as expected from the spin of the electron. Its value depends on the cuts by which the quantum mechanical region is removed and finally on the real path on which the charge is moving.

The mean electric field of the synchrotron radiation reproduces the Coulomb field. The field is however not spherical symmetric but it dominates close to the plane of circulation.

The solution of the homogeneous wave equation describes the propagation of the electromagnetic waves in vacuum. This background field may be formed during the creation process of the charge and be maintained by the synchrotron radiation of the charge. When evaluated in a spherical coordinate system it leads to a central radiation background with a special solution which moves in φ -direction but with standing waves in ϑ and r .

The central wave field can carry the massless charge on tracks around the origin. It generates smooth electric field lines e.g. a circular one but in general these are oscillating in space. The charge tries to follow these field lines by emitting synchrotron radiation and this radiation is guided back by the central wave and forms a feed back system which compensates the energy loss in φ -direction. Fast oscillations will be damped and the interaction will select the configuration with the lowest energy.

The standing wave of the background field in r -direction for the special solution of $m = 1$ extends to infinity and leads to an infinite total angular momentum and an infinite total energy of the central wave. A 2-dimensional Fourier like expansion of the wave functions in φ and x may form a finite solution. An admixture of an $m = 3$ contribution leads already to a finite angular momentum and an example of a Fourier-Bessel like expansion in x lead to a finite energy too.

The synchrotron radiation bucket moves with $\beta = 1$. The inner tensions which normally occur at lower speed if one cuts out the singularity disappear now. A constant mass energy compatible with the relativistic energy-momentum tensor of the field results.

Thus one finds, that the electron may totally be described by the synchrotron radiation of a massless charge field. It does not only behaves like a wave, it is a wave.

APPENDIX

Solving the homogeneous wave equation in spherical coordinates

The wave equation

$$\vec{curl} \vec{curl}(\vec{\mathcal{F}}) = -\frac{1}{c^2} \frac{\partial^2 \vec{\mathcal{F}}}{\partial t^2} \quad (48)$$

is solved in spherical coordinates for a vector field $\vec{\mathcal{F}}$ to yield directly the spherical components of the field. The equation is

expected to separate in the variables when a product ansatz is made, e.g. for \mathcal{F}_r :

$$\mathcal{F}_r = A_r \cdot \mathcal{R}_r(x) \cdot \Theta_r(\vartheta) \cdot \Phi_r(\varphi) \cdot \mathcal{T}(t) \quad (49)$$

and with

$$\begin{aligned} \mathcal{T}(t) &= e^{\pm i\omega t} \quad \text{and} \\ \Phi(\varphi) &= e^{\pm im\varphi}, \quad k = \omega/c, \quad kr = x. \end{aligned} \quad (50)$$

One expects a source free wave field and may thus subtract $\vec{\nabla}(\vec{\nabla}\mathcal{F})$ in eqn. (48) as one does in Cartesian coordinates. This simplifies the equation, but has to be checked afterwards. The ansatz eqn. (50) eliminates the time and φ -dependence in the equation and the 3 following components remain:

$$\left[\begin{array}{l} -A_r \Theta_r(\vartheta) \frac{\partial}{\partial x} \frac{1}{x^2} \frac{\partial}{\partial x} x^2 R_r(x) \\ -A_r \frac{R_r(x)}{x^2 \sin(\vartheta)^2} \Theta_r(\vartheta) \\ \cdot (x^2 \sin(\vartheta)^2 - m^2) \\ -A_r \frac{R_r(x)}{x^2 \sin(\vartheta)} \frac{\partial}{\partial \vartheta} \sin(\vartheta) \frac{\partial}{\partial \vartheta} \Theta_r(\vartheta) \\ A_\vartheta \frac{2R_\vartheta(x)}{x^2} \\ \cdot \left(\frac{\cos(\vartheta)}{\sin(\vartheta)} \Theta_\vartheta(\vartheta) + \frac{\partial}{\partial \vartheta} \Theta_\vartheta(\vartheta) \right) \\ + A_\varphi 2m \frac{R_\varphi(x)}{x^2 \sin(\vartheta)} \Theta_\varphi(\vartheta) \end{array} \right] = 0, \quad (51)$$

$$\left[\begin{array}{l} 2A_r R_r(x) \frac{\partial}{\partial \vartheta} \Theta_r(\vartheta) \\ + A_\vartheta \Theta_\vartheta(\vartheta) \frac{\partial}{\partial x} x^2 \frac{\partial}{\partial x} R_\vartheta(x) \\ + A_\vartheta R_\vartheta(x) \\ \cdot \frac{\partial}{\partial \vartheta} \frac{1}{\sin(\vartheta)} \frac{\partial}{\partial \vartheta} \sin(\vartheta) \Theta_\vartheta(\vartheta) \\ - A_\vartheta R_\vartheta(x) \Theta_\vartheta(\vartheta) \left(\frac{m^2}{\sin(\vartheta)^2} - x^2 \right) \\ - 2mA_\varphi R_\varphi(x) \frac{\cos(\vartheta)}{\sin(\vartheta)^2} \Theta_\varphi(\vartheta) \end{array} \right] = 0, \quad (52)$$

$$\left[\begin{array}{l} 2A_r R_r(x) \Theta_r(\vartheta) \frac{m}{\sin(\vartheta)} \\ + 2mA_\vartheta R_\vartheta(x) \frac{\cos(\vartheta)}{\sin(\vartheta)^2} \Theta_\vartheta(\vartheta) \\ - A_\varphi \Theta_\varphi(\vartheta) \frac{\partial}{\partial x} x^2 \frac{\partial}{\partial x} R_\varphi(x) \\ - A_\varphi R_\varphi(x) \frac{1}{\sin(\vartheta)} \\ \cdot \frac{\partial}{\partial \vartheta} \sin(\vartheta) \frac{\partial}{\partial \vartheta} \Theta_\varphi(\vartheta) \\ + A_\varphi R_\varphi(x) \Theta_\varphi(\vartheta) \left(\frac{m^2+1}{\sin(\vartheta)^2} - x^2 \right) \end{array} \right] = 0. \quad (53)$$

One obtains special solutions if one chooses

$$R_\vartheta(x) = j_{n\vartheta 1}(x) + a_\vartheta \frac{j_{n\vartheta 1+1}(x)}{x} \quad (54)$$

$$R_\varphi(x) = j_{n\varphi 1}(x) + a_\varphi \frac{j_{n\varphi 1+1}(x)}{x}$$

$$\Theta_r(\vartheta) = P_p^q(\vartheta)$$

$$\Theta_\vartheta(\vartheta) = P_p^q(\vartheta) \quad (55)$$

$$\Theta_\varphi(\vartheta) = P_p^q(\vartheta))$$

and uses

$$\frac{1}{\sin(\vartheta)} \frac{\partial}{\partial \vartheta} \sin(\vartheta) \frac{\partial}{\partial \vartheta} P_n^m(\vartheta) \quad (56)$$

$$= \left[\frac{m^2}{\sin(\vartheta)^2} - n(n+1) \right] P_n^m(\vartheta),$$

$$\frac{\partial}{\partial x} x^2 \frac{\partial}{\partial x} j_n(x) = [n(n+1) - x^2] j_n(x).$$

If one eliminates $R_r(x)$ from both eq. (52) and eq. (53), and sets $n\vartheta = n\varphi$ one arrives at

$$\left[\begin{array}{l} \frac{mP_\nu^m(\vartheta)}{\sin(\vartheta)\frac{\partial}{\partial\vartheta}P_\nu^m(\vartheta)} \\ A_\vartheta\left(\frac{\partial}{\partial x}x^2\frac{\partial}{\partial x}R_\vartheta(x)\right)P_\nu^\mu(\vartheta) \\ A_\vartheta R_\vartheta(x) \\ \cdot \frac{\partial}{\partial\vartheta}\frac{1}{\sin(\vartheta)}\frac{\partial}{\partial\vartheta}\sin(\vartheta)P_\nu^\mu(\vartheta) \\ -A_\vartheta R_\vartheta(x)P_\nu^\mu(\vartheta) \\ \cdot \left(\frac{m^2}{\sin(\vartheta)^2} - x^2\right) \\ -2A_\varphi mR_\varphi(x)\frac{\cos(\vartheta)}{\sin(\vartheta)^2}P_L^M(\vartheta) \\ \left[\begin{array}{l} 2mA_\vartheta R_\vartheta(x)P_\nu^\mu(\vartheta)\frac{\cos(\vartheta)}{\sin(\vartheta)^2} \\ -A_\varphi\left(\frac{\partial}{\partial x}x^2\frac{\partial}{\partial x}R_\varphi(x)\right)P_L^M(\vartheta) \\ +A_\varphi R_\varphi(x)P_L^M(\vartheta)\left[\frac{m^2-M^2+1}{\sin(\vartheta)^2}\right. \\ \left.+L(L+1)-x^2\right] \end{array} \right] \end{array} \right] = 0. \quad (57)$$

One gets now 2 solutions for eq. (57). One for which both the upper and lower cluster vanish separately, and the other one for which the left side of this equation vanishes on the whole.

When these results are inserted into equ. (51) they determine $R_r(x)$, and $\text{div}(\vec{\mathcal{F}}) = 0$ restricts the values of the separation constants. Both solutions may represent solutions of the electromagnetic fields $\vec{\mathcal{E}}$ and $\vec{\mathcal{H}}$.

ACKNOWLEDGMENT

A presentation of an early version of this paper to E. Lohrmann showed the regions which have to be further deepened. I am grateful to K. Fredenhagen for many detailed discussions. Without the patience and the confidence of my wife Ursula this work would not exist.

REFERENCES

- [1] A. O. Barut, *Brief History and Recent Developments in Electron Theory and Quantumelectrodynamics in The Electron New Theory and Experiment* (D. Hestenes and A. Weingart, Editors; Springer, 1991) p. 105
- [2] L. de Broglie, *Nonlinear Wave Mechanics* (Elsevier, Amsterdam 1960) p. 6
- [3] J. Orear, *Jay Orear Physics* (Macmillan, New York 1979)) Chp. 18-4
- [4] M. Alonso, E.J. Finn, *Fundamental University Physics II* (Addison-Wesley, Amsterdam 1974) 515
- [5] M. H. McGregor, *The Enigmatic Electron* (Kluwer Academic, Dordrecht 1992)
- [6] A. Sommerfeld, *Electrodynamics: Lectures on Theoretical Physics* (Academic Pr., New York 1952) §33
- [7] P. A. M. Dirac, Proc. Roy. Soc. London **A268**, (1962) 57
- [8] H. Jehle, Phys. Rev. **D15**, (1977) p. 3727 and citations there.
- [9] A. O. Barut and N. Zanghi, Phys. Rev. Lett. **52**, (1984) 2009
- [10] Qiu-Hong Hu, Physics Essays, **17**, (2004) 442
- [11] J. G. Williamson and M.B. van der Mark, Ann. de la Fondation Louis de Broglie **22**, (1997) 133
- [12] L. D. Landau and E. M. Lifshitz *The Classical Theory of Fields* (Butterworth-Heinemann, Oxford 2000) **2**, Chp. 8
- [13] *Handbook of Mathematical Functions* (editors: M. Abramovitz and I.A. Stegun; National Bureau Std., Appl. Math. Series 55, Washington 1966) Chp. 8, Chp. 10
- [14] P. M. Morse and H. Feshbach, *Methods of Theoretical Physics* (McGraw-Hill, New York 1953) Chp. 10, Chp. 11
- [15] D. Iwanenko and A. Sokolov *Klassische Feldtheorie* (Akademie-Verlag, Berlin 1953) §39
- [16] W. Greiner *Classical Electrodynamics* (Springer New York 1996) §21
- [17] J. D. Jackson *Classical Electrodynamics* (Wiley, New York 1975) Chp. 14
- [18] J. D. Jackson *ibid.* Chp. 16
- [19] I. N. Sneddon *Special Functions of Mathematical Physics and Chemistry* (Oliver and Boyd, Edinburgh 1961) §35
- [20] A. Sommerfeld, *Partial Differential Equations In Physics: Lectures On Theoretical Physics* (Academic Pr., New York 1952) §20, and exercise V.1
- [21] [17] Chp. 17
- [22] [15] §29 - §30
- [23] R. U. Sexl and H. K. Urbantke *Relativity, Groups, Particles* (Springer, Wien 2001) Chp. 5.10